nature biotechnology

Supplementary information

https://doi.org/10.1038/s41587-025-02761-2

# Target sequence-conditioned design of peptide binders using masked language modeling

In the format provided by the authors and unedited

## Table of Contents

### Supplementary Figures



### Supplementary Tables

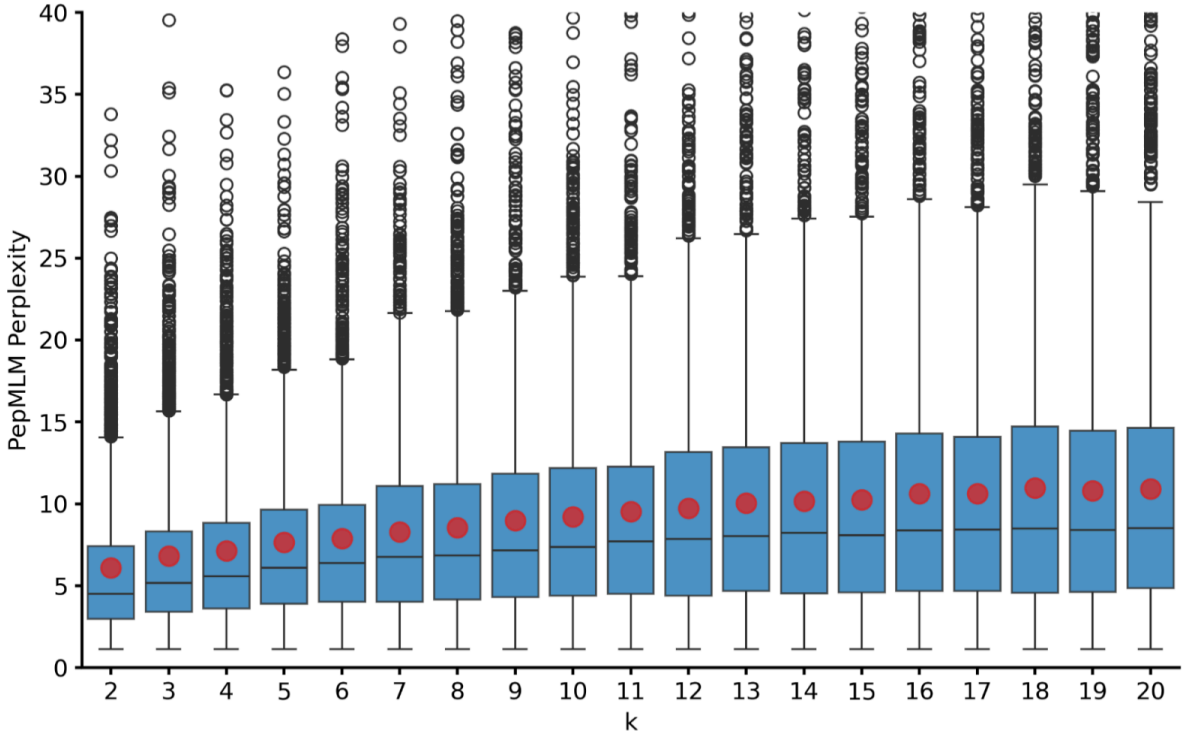


**Supplementary Figure 1. Top-*k* sampling and perplexity.** This figure illustrates the correlation between selected k values and the resulting Perplexity when generating binder sequences for target proteins, where each k value corresponds to the generation of 100 binders with lengths equating to the reference binder. The red point refers to the average PPL score. As k escalates, there is a corresponding increase in Perplexity, indicating reduced model confidence. At k=3, the model maintains a lower Perplexity, signifying higher reliability in its predictions. The choice of k=3 is supported not only by this enhanced assurance but also by considerations of diminishing returns; beyond this point, the gain in diversity is outweighed by the increase in complexity and the potential for atypical predictions. Moreover, practical considerations favor k=3, as it offers computational efficiency without compromising the diversity necessary for effective binder design. Consequently, k=3 is endorsed as the optimal value to achieve a balance between model confidence, diversity of binder sequences, and computational pragmatism.

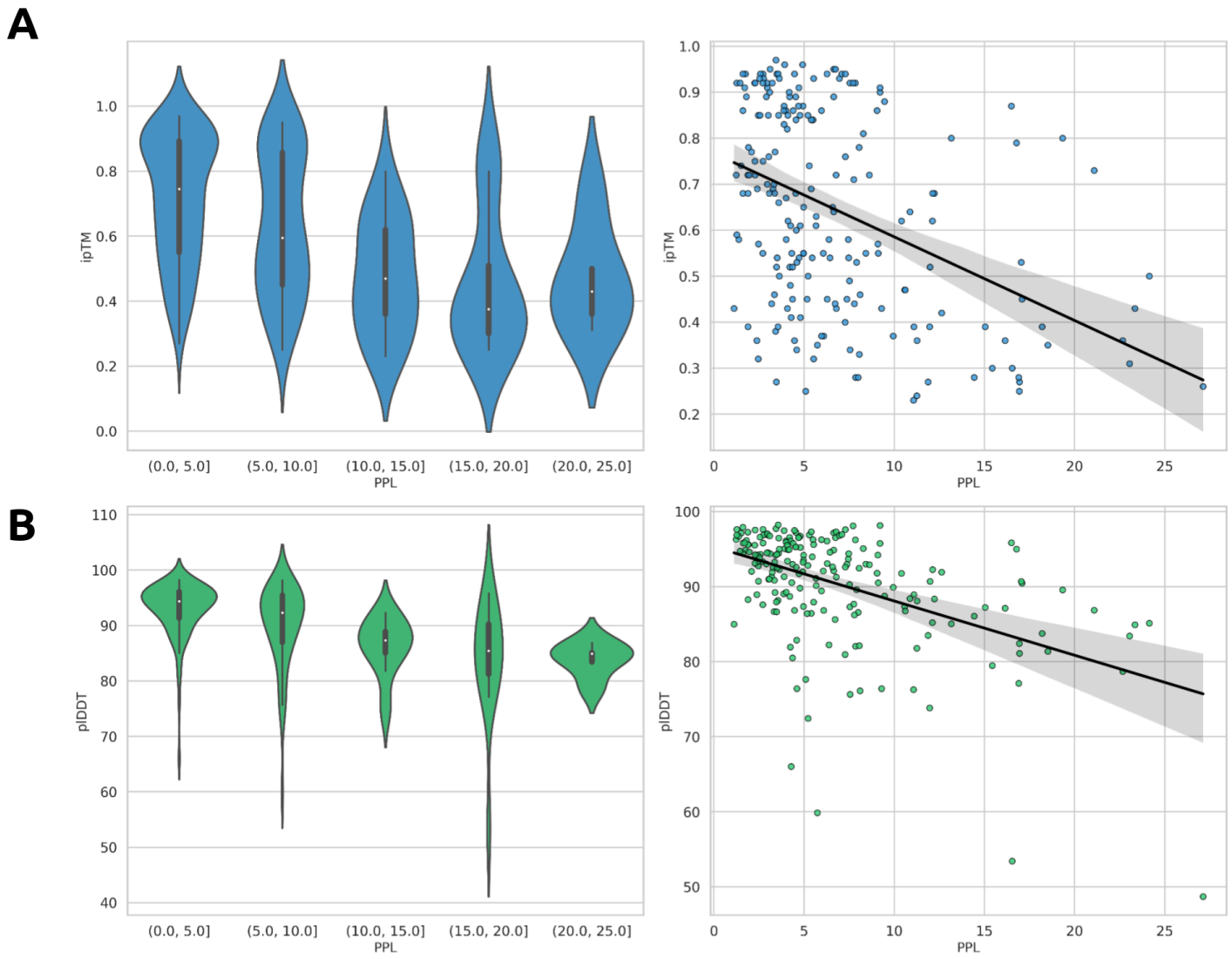


**Supplementary Figure 2. Association between model perplexity and co-folding metrics.** (A) Relationship between ipTM and perplexity (PPL). The initial segment of Figure A presents a violin plot, categorizing perplexity in 5-unit intervals. The subsequent segment delineates the raw data points, accompanied by a regression analysis, indicating a negative correlation (Pearson correlation coefficient -0.414, $p < 0.001$). The shaded area represents a 95% confidence interval. (B) Negative correlation between PPL and pLDDT, identified by Pearson correlation coefficient of -0.490 ($p < 0.001$). The violin plot underscores a marked decrement in specific folding metrics, most pronounced in ipTM, commensurate with elevated perplexity levels.

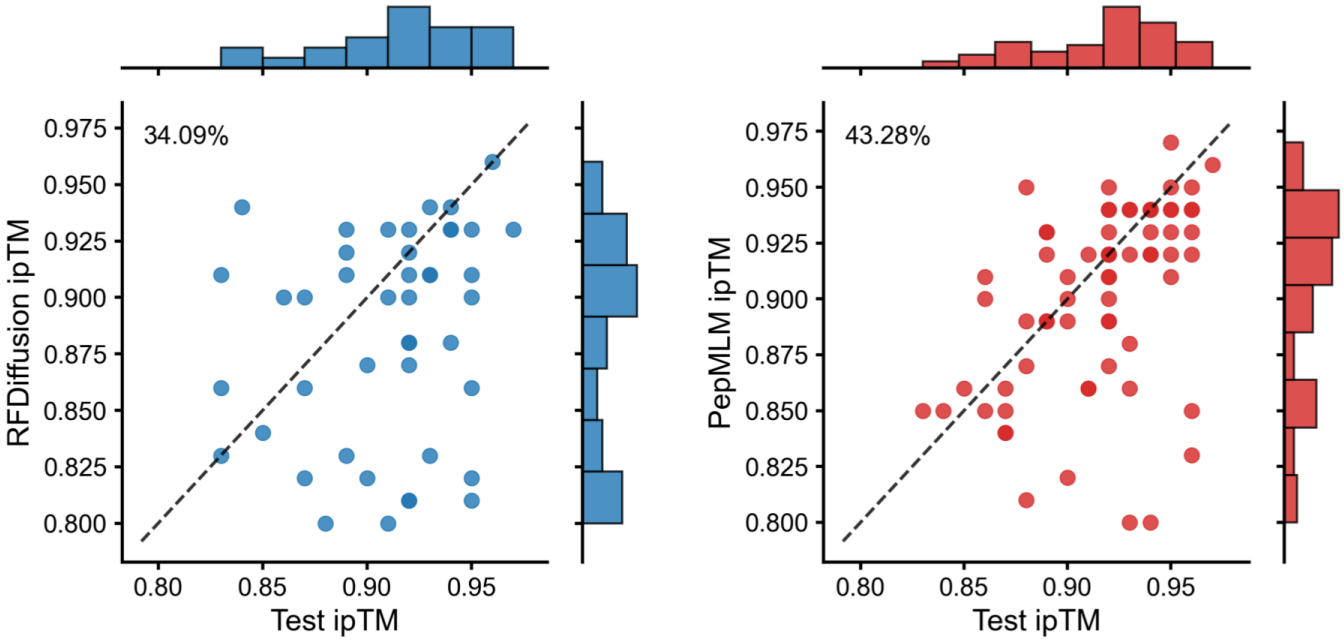


**Supplementary Figure 3. Benchmark RFDiffusion and PepMLM with high pLDDT filter.** Hit rate comparison between PepMLM and RFDiffusion generated binders after applying plDDT filter (> 0.8). PepMLM achieved a 43% hit rate compared to RFDiffusion's 34%.

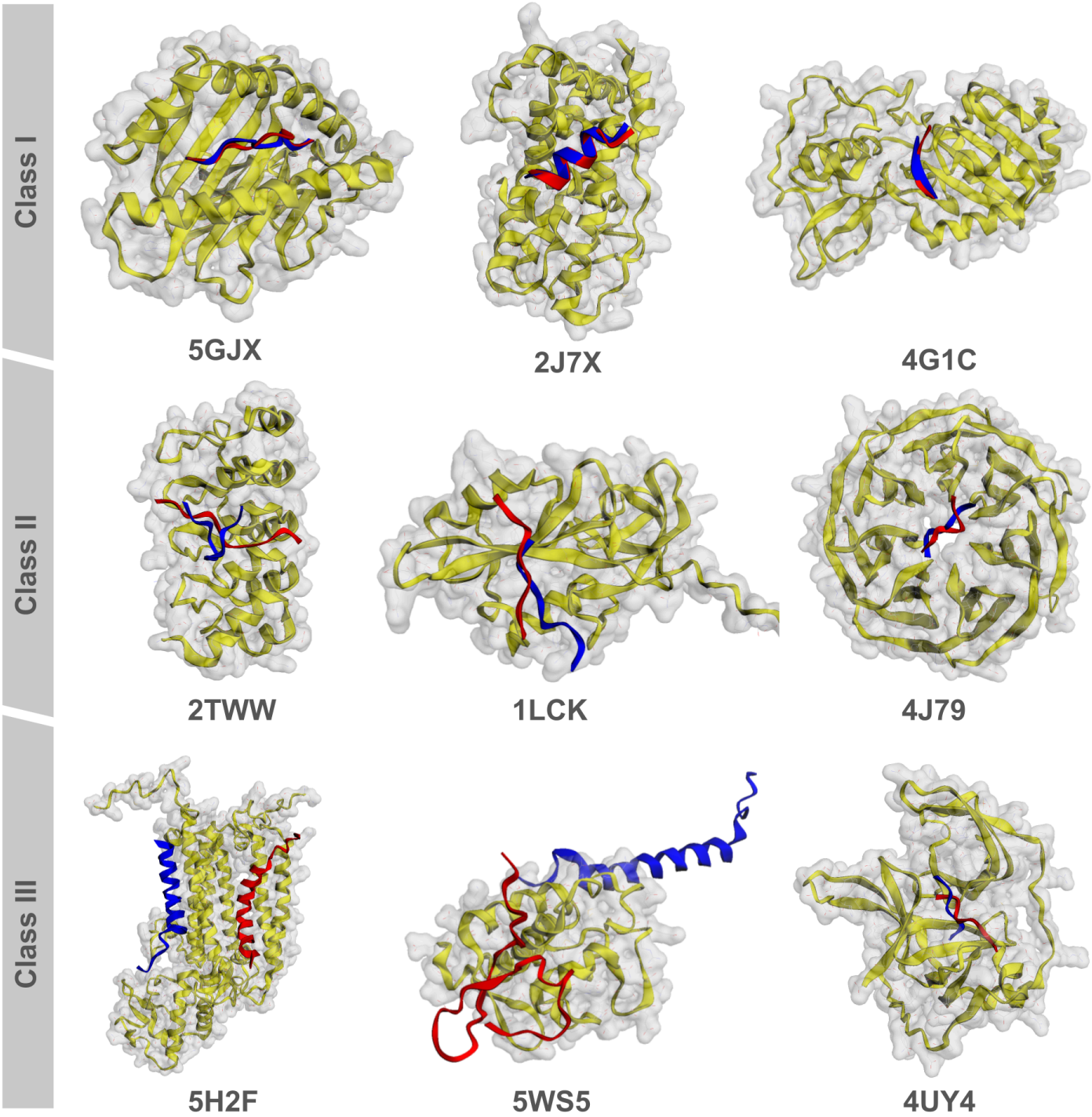


**Supplementary Figure 4. Visualization of binder-protein complexes.** Co-folded binder-protein complexes are categorized into three distinct classes for visualization purposes. Class I includes complexes where both the generated and test binders exhibit ipTM scores ≥ 0.7, Class II encompasses those with generated binders having ipTM scores ≥ 0.7 and test binders with ipTM scores < 0.7, and Class III contains complexes with both generated and test binders having ipTM scores ≤ 0.7. In these representations, the target protein is depicted in yellow, while the PepMLM-generated binders and test binders are illustrated in red and blue, respectively. This classification facilitates a detailed comparison of the structural relationships and binding patterns among the different classes of binder-protein complexes.

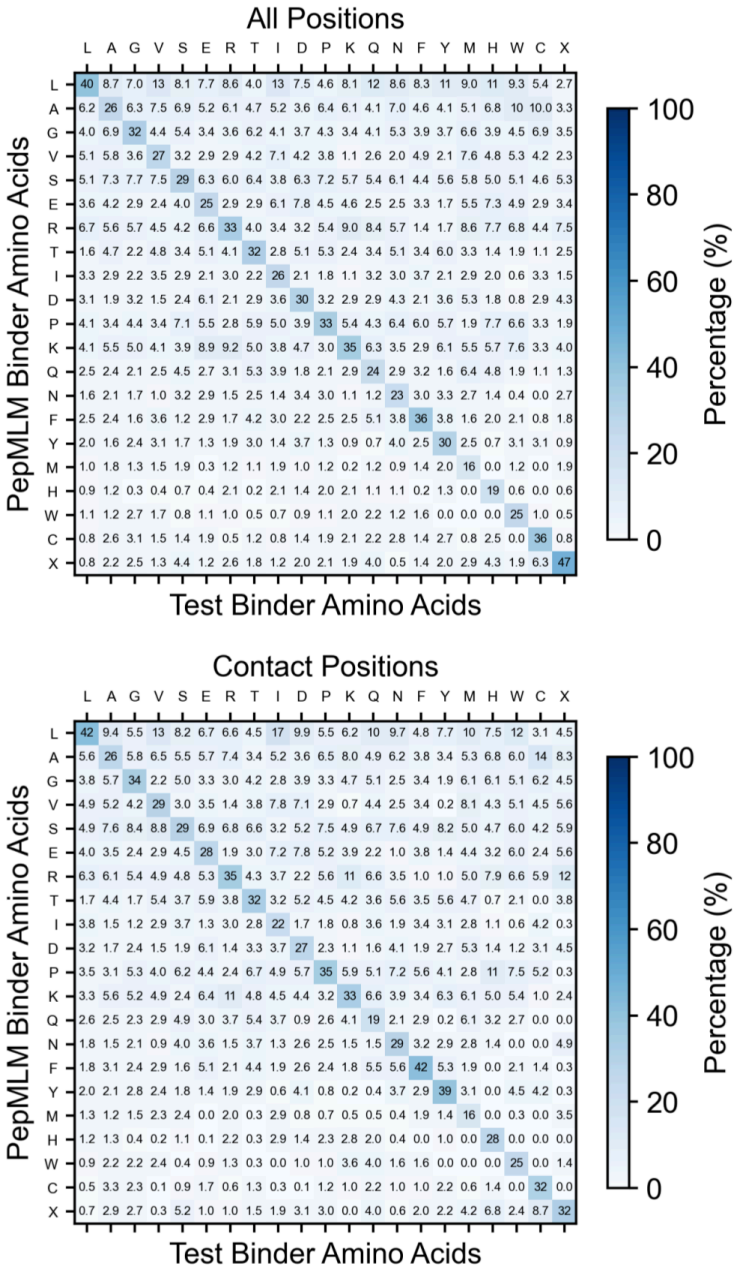


**Supplementary Figure 5. Amino acid specific generation matrix for all positions and contact positions.** (Top) Generation percentage across all positions for each AA, with rows representing amino acids in test binders and columns showing corresponding amino acids in generated binders (n=100 generations per test binder). (Bottom) Generation percentage specifically for contact positions, defined using an 8Å distance threshold. Color intensity indicates substitution frequency, with diagonal elements representing conservation of original amino acids. Position-specific changes of 69.2% and 68.4% were observed for all positions and contact positions, respectively.

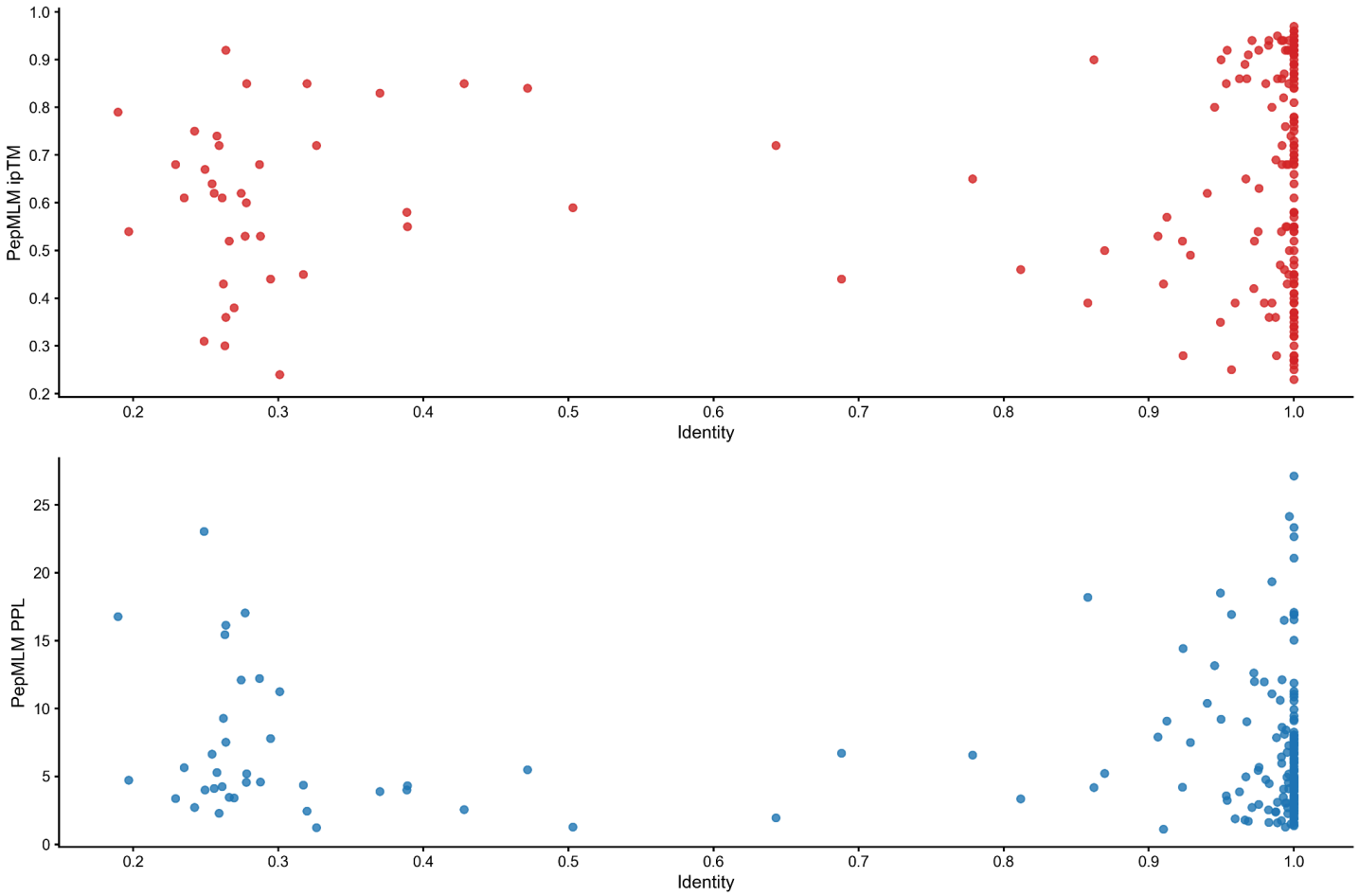


**Supplementary Figure 6. Identity, ipTM, and PPL scatter plot.** (Top) Relationship between maximum sequence identity of test targets against training set and AlphaFold-predicted ipTM scores of generated binders. The x-axis shows the maximum sequence identity computed using biotite Alignment, while the y-axis represents the predicted ipTM scores for PepMLM-generated binders. (Bottom) Relationship between maximum sequence identity and PPL scores. The x-axis maintains the same sequence identity metric, while the y-axis shows the PPL scores for generated binders. Scatter points represent individual target-binder pairs.

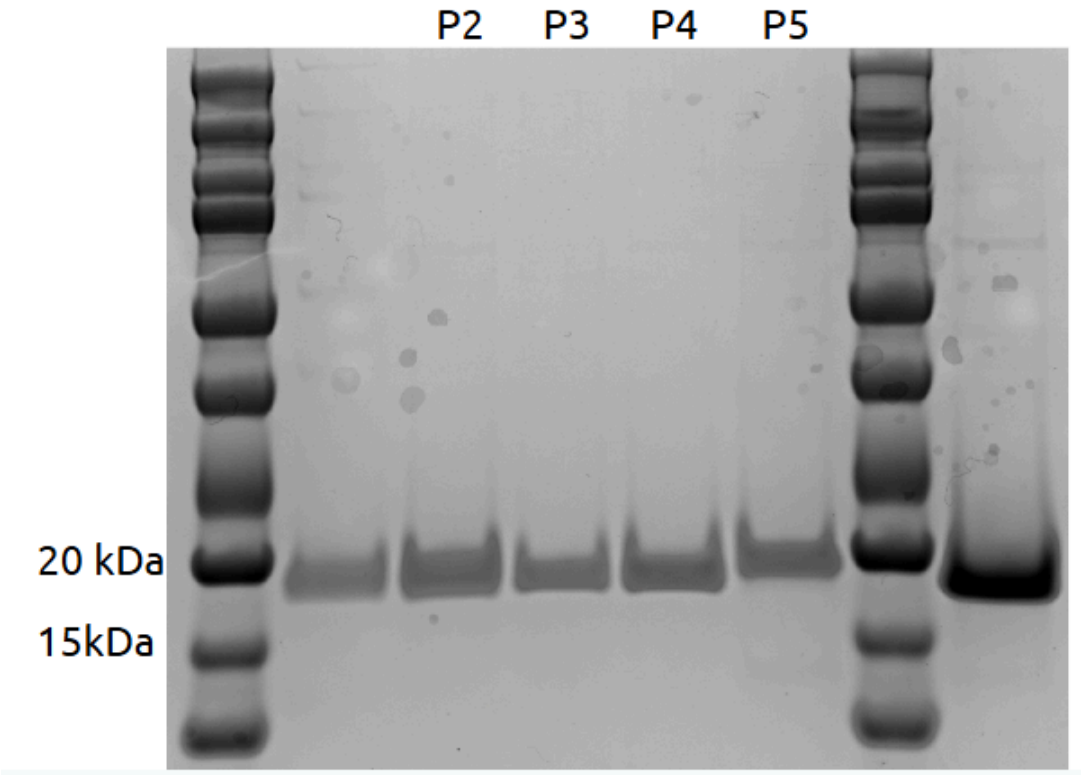


**Supplementary Figure 7. Representative coomassie-stained sodium dodecyl sulfate polyacrylamide gel electrophoresis (SDS-PAGE) of anti-AMHR2 SUMO-tag peptide constructs.** While constructs have a predicted molecular weight of 14.2 kDa based on amino acid sequence, the addition of a SUMO-tag fusion results in a higher apparent molecular weight of around 20 kDa.

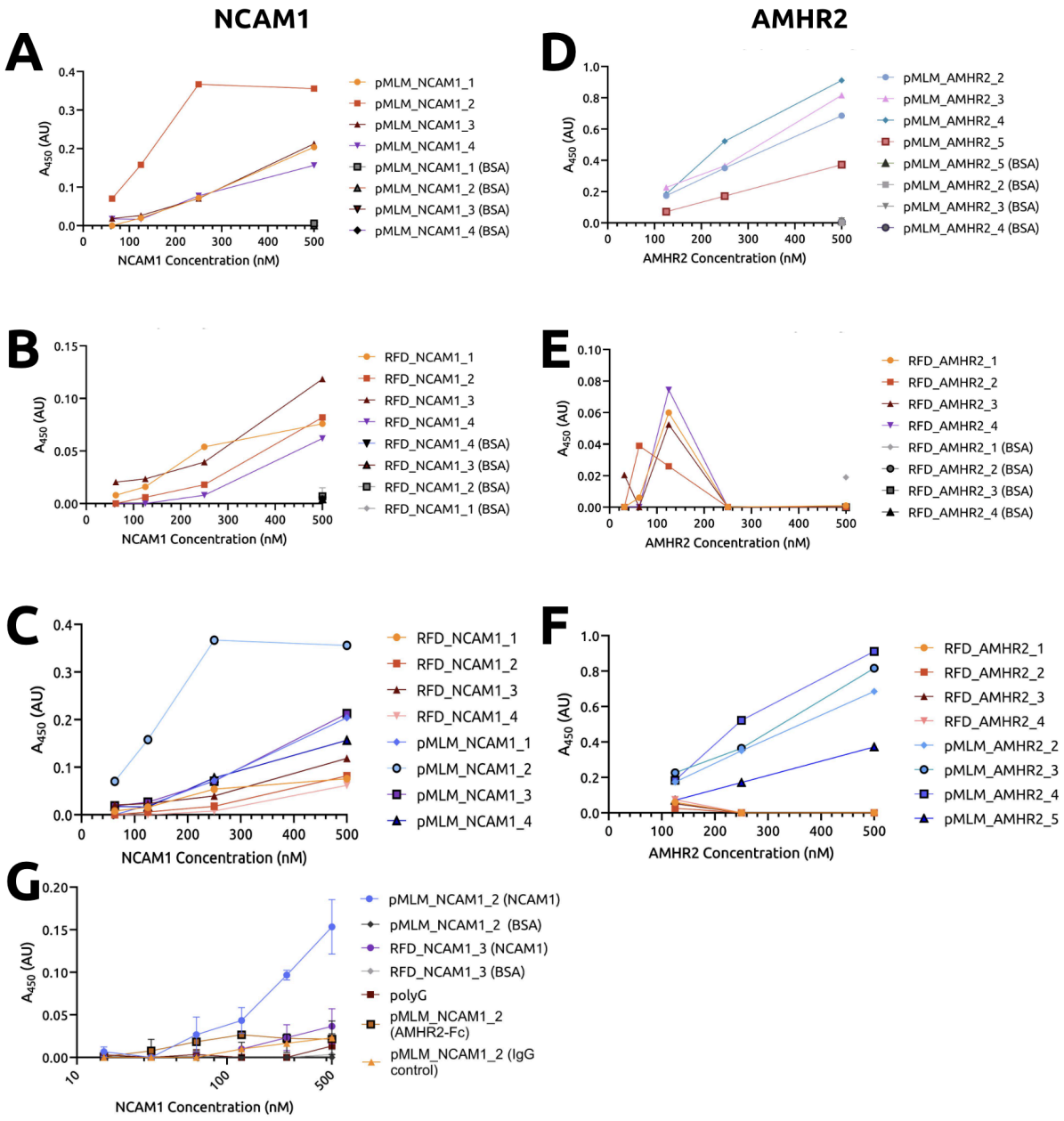


**Supplementary Figure 8. Preliminary ELISA screen of anti-AMHR2 binders and anti-NCAM1 peptide binders.** Four NCAM1-targeting peptides (N were generated for both RFDiffusion and PepMLM as C-terminal SUMO-tag fusions and screened for potential binding to NCAM1-Fc and AMHR2-Fc by ELISA (Supplementary Figure 8). Limited dilutions of each antigen were tested and 500 nM BSA was used as a control antigen. (A) Binding analysis of four potential PepMLM-generated anti-NCAM1 peptides (B) Binding analysis of four potential RFDiffusion-generated anti-NCAM1 peptides (C) PepMLM and RFDiffusion screens from A and B plotted on the same axes. (D) Binding analysis of four potential PepMLM-generated anti-AMHR2 peptides (E) Binding analysis of four potential RFDiffusion-generated anti-AMHR2 peptides. (F) PepMLM and RFDiffusion screens from D and E plotted on the same axes. (G) Binding analysis of top candidate peptide against NCAM1 for each algorithm fused to C-terminal SUMO-tag as measured by ELISA. PepMLM-designed peptides were immobilized onto 96-well plates, incubated with serial dilutions of either NCAM1-Fc or BSA, and subsequently detected with an anti-IgG-HRP conjugate. An anti-NCAM1 antibody and AMHR2-Fc was used as IgG control. For preliminary screens (A-F). Data are single point measurements (besides blanks) and each absorbance signal is subtracted by the average of its associated blank values (in duplicate). Axes for subplots A-F are linear, the axis of subplot G is log(concentration). No outliers were removed.

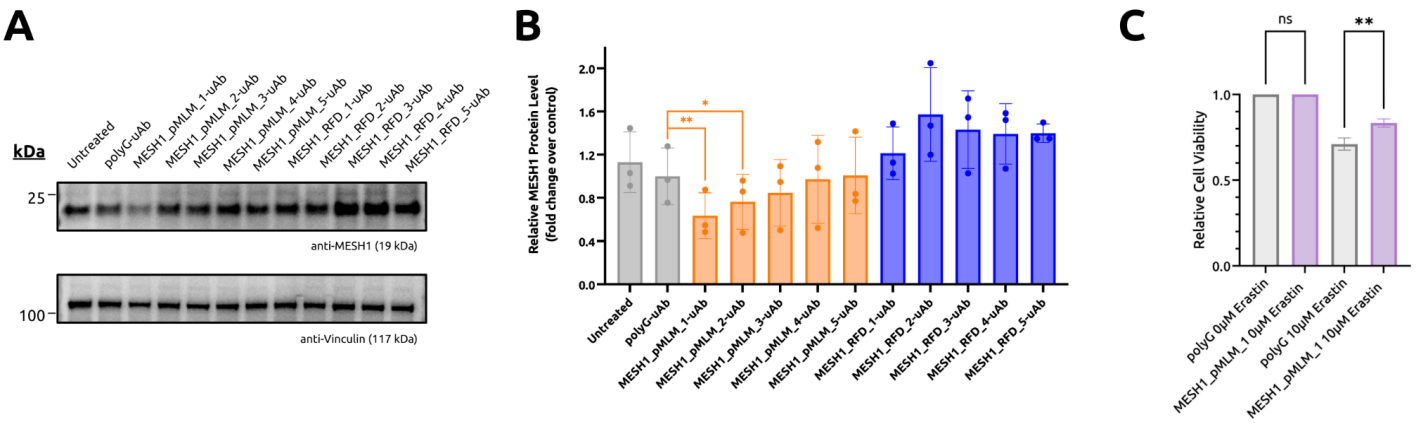


**Supplementary Figure 9. PepMLM-generated uAb degraders of MESH1.** A) Western blot analysis of HeLa cell lysate post-transfection of uAb vectors. polyG-uAb was used as a transfection control and Vinculin was used as the loading control. B) Densitometry analysis of accompanying Western blots, normalized to polyG and Vinculin controls. Statistical significance is determined by a paired one-tailed Student's t test. Calculated p values are represented as follows: **p < 0.01; ***p < 0.001). C) Inhibition of ferroptosis-related cell death upon transfection of anti-MESH1 uAbs into HEK293T cells in the presence of erastin.

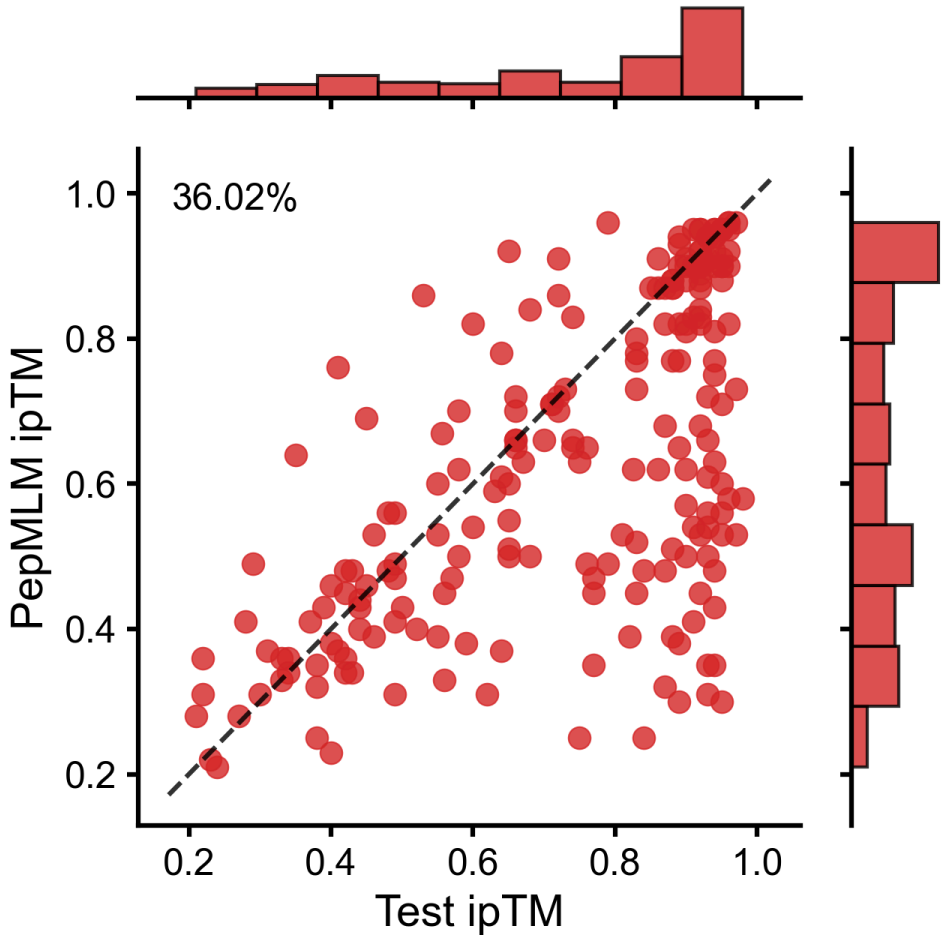


**Supplementary Figure 10. Evaluation of PepMLM-3B.** *In silico* hit-rate assessment. Utilizing AlphaFold-Multimer, the ipTM scores were computed for both the generated and test peptides in conjunction with the target protein sequence. The entries are organized in accordance with the ipTM scores attributed to the test set peptides. The hit rate is characterized by the generated peptides exhibiting ipTM scores ≥ those of the test set peptides.

**Supplementary Table 1. Settings and hyperparameters used to train PepMLM-650M.**

| Name | Setting |
|---|---|
| Learning Rate | 0.000798 |
| Batch Size | 16 |
| Gradient Accumulation | 2 |
| Warm up steps | 501 |
| Number of training epochs | 5 |
| Optimizer | AdamW (default) |
| Trainer | Default HuggingFace Settings |

**Supplementary Table 2. Outlier analysis of protein-peptide complexes**. This table displays 12 protein-peptide complexes with pseudo-perplexity (PPL) values exceeding 40. Included are evaluation metrics for both the test complexes and the PepMLM generation results, as well as the binder sequences. ipTM scores for test and generated complexes are highlighted in different colors for comparison. Notably, even though these outliers exhibit high PPL values indicative of accurate modeling by PepMLM, the model remains proficient in generating binders that perform equivalently well *in silico* as per AlphaFold-Multimer ipTM score.

| | Test | | | | PepMLM Generation | | | |
|---|---|---|---|---|---|---|---|---|
| **PDB ID** | **Binder** | **PPL** | **ipTM** | **pLDDT** | **Binder** | **PPL** | **ipTM** | **pLDDT** |
| 5B5V | FLFGSRSS | 42.8 | 0.45 | 88.9 | YHYVMRYA | 4.2 | 0.52 | 88.7 |
| 4G1C | AVXCAX | 82.5 | 0.86 | 97.0 | TAKXST | 3.0 | 0.91 | 96.9 |
| 2L1C | RAKWDTANNPLXKE ATSTFTNITXRGT | 45.4 | 0.49 | 61.9 | HIAEEPHFFESMQN NYEKPTTYKFQQK | 12.0 | 0.39 | 73.8 |
| 6GHJ | FAQ | 209.7 | 0.71 | 93.4 | MXL | 3.4 | 0.68 | 93.3 |
| 6AMU | MMWDRGLGMM | 59.2 | 0.34 | 87.9 | YQALIGGFNA | 14.4 | 0.28 | 86.1 |
| 5WMR | QIKVRVDMV | 76.3 | 0.91 | 92.3 | LRFWRARTL | 9.0 | 0.86 | 91.8 |
| 5NJC | VLEDRI | 63.0 | 0.83 | 97.5 | AAAAAA | 1.5 | 0.74 | 97.1 |
| 5FML | LSNDISQGIKRQRM TVESM | 42.8 | 0.91 | 94.0 | AAMTKLALAAKTRA QLFKK | 16.1 | 0.36 | 87.1 |
| 6DQU | GIINTL | 65.8 | 0.87 | 97.7 | YLGANG | 5.4 | 0.84 | 97.3 |
| 2IWB | GHMS | 194.0 | 0.64 | 96.1 | XPPX | 4.0 | 0.67 | 95.9 |
| 4MLI | AHIVMVDAYKPT | 62.6 | 0.87 | 97.5 | GPTPVQVLKRRG | 17.0 | 0.53 | 90.7 |
| 5DHM | RSIEISIRVDDFTKTG ETVRY | 64.2 | 0.93 | 94.4 | AQSPEIITADVVVTS DEFTTT | 19.3 | 0.8 | 89.6 |

**Supplementary Table 3. Sequence information and folding metrics for complexes in Supplementary Figure 4.**

| PDB ID | Generated Binder | plDDT | ipTM | Test Binder | plDDT | ipTM | Target Identity | Binder Identity |
|---|---|---|---|---|---|---|---|---|
| 5GJX | RLLEWMIYI | 96.3 | 0.92 | RLIQNSITI | 96.0 | 0.92 | 0.99 | 0.44 |
| 2J7X | HHLLLHLLTQD | 91.9 | 0.92 | IQSLINLLADN | 91.9 | 0.91 | 0.99 | 0.28 |
| 4G1C | TAKXST | 96.9 | 0.91 | AVXCAX | 97.0 | 0.86 | 0.99 | 0.15 |
| 3TWW | RREPPGGAFRX | 97.4 | 0.87 | RQSPDGQSFRX | 92.7 | 0.48 | 0.99 | 0.55 |
| 1LCK | PPXEEIPP | 87.3 | 0.92 | EGQQPQPA | 86.1 | 0.68 | 0.60 | 0.13 |
| 4J79 | AARHLD | 97.3 | 0.72 | EKVHVQ | 97.2 | 0.64 | 0.99 | 0.17 |
| 5H2F | XETNTLVRYVVAHFVLLVSVILIREAPRIESSKXX | 84.9 | 0.43 | XETITYVFIFACIIALFFFAIFFREPPRITXXXXX | 86.7 | 0.27 | 0.93 | 0.4 |
| 5WS5 | SSEEGRPILWIATTTGGGGVIIIVLFLFYAYYGSLSXLXXX | 77.7 | 0.24 | MSEGGRIPLWIVATVAGMGVIVIVGLFFYGAYAGLGSSLXX | 86.4 | 0.24 | 0.99 | 0.48 |
| 4UY4 | ARTKQT | 90.1 | 0.63 | ARTXQT | 89.0 | 0.43 | 0.97 | 0.83 |

**Supplementary Table 4. Peptide sequences and PPL scores for experimental testing.** The accession IDs for NCAM1, MSH3, and HTT are from UniProt. Viral target sequences are derived from NCBI/GenBank accession IDs.

| Target | Accession ID | uAb Name | Peptide Sequence | Derivation Algorithm | PPL |
|---|---|---|---|---|---|
| **Figure 2** | | | | | |
| NCAM1 | P13591 | NCAM1_pMLM_1 | GKLPLPSLPCK | PepMLM | 5.343684945 |
| NCAM1 | P13591 | NCAM1_pMLM_2 | GLGPSPVLPRC | PepMLM | 5.299030403 |
| NCAM1 | P13591 | NCAM1_pMLM_3 | GLGPLPVLPCK | PepMLM | 6.329989946 |
| NCAM1 | P13591 | NCAM1_pMLM_4 | HSLGQPLSPIC | PepMLM | 4.753515747 |
| NCAM1 | P13591 | NCAM1_RFD_1 | SLPIENIYIEA | RFDiffusion | N/A |
| NCAM1 | P13591 | NCAM1_RFD_2 | MKPIEVVYEKA | RFDiffusion | N/A |
| NCAM1 | P13591 | NCAM1_RFD_3 | ELPEQVIYIEA | RFDiffusion | N/A |
| NCAM1 | P13591 | NCAM1_RFD_4 | EKPIEVIYEKA | RFDiffusion | N/A |
| AMHR2 | Q16671 | pMLM_AMHR2_2 | LTRYTSLAAQGC | PepMLM | 13.09 |
| AMHR2 | Q16671 | pMLM_AMHR2_3 | DTTLYSGFAQYG | PepMLM | 13.48 |
| AMHR2 | Q16671 | pMLM_AMHR2_4 | DESLRSFLAHYC | PepMLM | 15.31 |
| AMHR2 | Q16671 | pMLM_AMHR2_5 | LETYRSGLAQYC | PepMLM | 16.09 |
| AMHR2 | Q16671 | RFD_NCAM_1 | APAVTGSILADL | RFDiffusion | N/A |
| AMHR2 | Q16671 | RFD_NCAM_2 | SAAVTGSILADL | RFDiffusion | N/A |
| AMHR2 | Q16671 | RFD_NCAM_3 | RSIRLSYPVELP | RFDiffusion | N/A |
| AMHR2 | Q16671 | RFD_NCAM_4 | RSVRLVHPVELP | RFDiffusion | N/A |
| **Figure 3** | | | | | |
| MSH3 | P20585 | MSH3_pMLM_1 | SRREQLARILEGAFLASK | PepMLM | 7.65 |
| MSH3 | P20585 | MSH3_pMLM_2 | SRLEESASAMEASAAQAS | PepMLM | 9.12 |
| MSH3 | P20585 | MSH3_pMLM_3 | SRLKQAKSIMGGSLLLAE | PepMLM | 9.61 |
| MSH3 | P20585 | MSH3_pMLM_4 | NRLVEALASLEFSAQLSE | PepMLM | 9.91 |
| MSH3 | P20585 | MSH3_pMLM_5 | SRNKELKSILEFSLAQQK | PepMLM | 11 |
| MSH3 | P20585 | MSH3_pMLM_6 | SRLKQLASALDGSFLQAS | PepMLM | 11.84 |

| | | | | | |
|---|---|---|---|---|---|
| MSH3 | P20585 | MSH3_pMLM_7 | SLRKELASAMEFAAAQSK | PepMLM | 12.24 |
| MSH3 | P20585 | MSH3_pMLM_8 | SLNEQAASILEAFFAQSS | PepMLM | 13.47 |
| MSH3 | P20585 | MSH3_pMLM_9 | SYNVELASISEASLAAAK | PepMLM | 13.69 |
| MSH3 | P20585 | MSH3_pMLM_10 | SLNEQLASIMGGSAQLAE | PepMLM | 14.11 |
| MSH3 | P20585 | MSH3_pMLM_11 | SRRVELLSILEFALAAAS | PepMLM | 14.45 |
| HTT (Q43) | P42858 | Q43_pMLM_1 | SAAPQLLGSGLALGK | PepMLM | **Q43:** 5.302052023 **Q17:** 21.74186374 |
| HTT (Q43) | P42858 | Q43_pMLM_2 | TAPQLSQASGLAGGK | PepMLM | **Q43:** 6.223211251 **Q17:** 22.05928384 |
| HTT (Q43) | P42858 | Q43_pMLM_3 | LAPQLLLLGLGGLAK | PepMLM | **Q43:** 6.122010055 **Q17:** 21.22001317 |
| HTT (Q43) | P42858 | Q43_pMLM_4 | SAPPQLAAAGGLLLA | PepMLM | **Q43:** 5.42110285 **Q17:** 19.667137 |
| HTT (Q43) | P42858 | Q43_pMLM_5 | SPPPQAAAGAALGAK | PepMLM | **Q43:** 6.196895246 **Q17:** 20.36823003 |
| **Figure 4** | | | | | |
| Hendravirus P | MN062017.1 | HeV_1 | RLPVYLSLQG | PepMLM | 3.635173 |
| Hendravirus P | MN062017.1 | HeV_2 | HSPVHLSLLG | PepMLM | 4.296802 |
| Hendravirus P | MN062017.1 | HeV_3 | SRSVLHSLLQGR | PepMLM | 4.974103 |
| Hendravirus P | MN062017.1 | HeV_4 | HSSVLQSLFGG | PepMLM | 5.449664 |
| Hendravirus P | MN062017.1 | HeV_5 | SESLYLSLFKG | PepMLM | 6.702855 |
| Hendravirus P | MN062017.1 | HeV_6 | SMSRRRQLAKKLLLLAIKS | PepMLM | 6.707319 |
| Hendravirus P | MN062017.1 | HeV_7 | RQSLRQQLLLDLGR | PepMLM | 6.74773 |
| Hendravirus P | MN062017.1 | HeV_8 | SSLVYLSLGA | PepMLM | 6.824329 |
| Hendravirus P | MN062017.1 | HeV_9 | HLSLPHSLLQKR | PepMLM | 6.850688 |
| Hendravirus P | MN062017.1 | HeV_10 | SMSVEKSLSKKLGKKLIKS | PepMLM | 6.855796 |
| Hendravirus P | MN062017.1 | HeV_11 | RSLVKKQLLLKLLG | PepMLM | 6.950253 |
| Hendravirus P | MN062017.1 | HeV_12 | MQSVKLKLLLKGLLR | PepMLM | 7.039044 |
| Hendravirus P | MN062017.1 | HeV_13 | HSSVLQQLFGE | PepMLM | 7.046471 |
| Hendravirus P | MN062017.1 | HeV_14 | HHSLLQSLLQGT | PepMLM | 7.287729 |

| | | | | | |
|---|---|---|---|---|---|
| Hendravirus P | MN062017.1 | HeV_15 | RLPLYLSLGA | PepMLM | 7.372559 |
| Hendravirus P | MN062017.1 | HeV_16 | HHSLLHSLLKGT | PepMLM | 7.621191 |
| Hendravirus P | MN062017.1 | HeV_17 | RLSVLQQLLKLGG | PepMLM | 7.758791 |
| Hendravirus P | MN062017.1 | HeV_18 | SLSRRQQLLLDLGK | PepMLM | 7.797618 |
| Hendravirus P | MN062017.1 | HeV_19 | SKPLYLLLGG | PepMLM | 7.82979 |
| Hendravirus P | MN062017.1 | HeV_20 | RLSVRKLLLLDLGK | PepMLM | 7.860104 |
| HMPV P | AAS22075.1 | HMPV_1 | LTLEQLQEKR | PepMLM | 6.510858 |
| HMPV P | AAS22075.1 | HMPV_2 | TLEEELLLKR | PepMLM | 7.514123 |
| HMPV P | AAS22075.1 | HMPV_3 | LTLEQLQLIR | PepMLM | 7.855078 |
| HMPV P | AAS22075.1 | HMPV_4 | AELLLRQQQLLL | PepMLM | 7.869746 |
| HMPV P | AAS22075.1 | HMPV_5 | SVLTAEQLIKI | PepMLM | 8.039237 |
| HMPV P | AAS22075.1 | HMPV_6 | DLRRRLAEKTPELQLLLI | PepMLM | 8.068756 |
| HMPV P | AAS22075.1 | HMPV_7 | ALLAKKLTLEALLAL | PepMLM | 8.235918 |
| HMPV P | AAS22075.1 | HMPV_8 | AEEAKKLTEELLRLR | PepMLM | 8.411599 |
| HMPV P | AAS22075.1 | HMPV_9 | DTELAAKKLTTELLLKI | PepMLM | 8.626335 |
| HMPV P | AAS22075.1 | HMPV_10 | TLTLQQLLKL | PepMLM | 8.713968 |
| HMPV P | AAS22075.1 | HMPV_11 | ADRLAALSLETRQALLKI | PepMLM | 9.022841 |
| HMPV P | AAS22075.1 | HMPV_12 | LLRLELSKLTAELALLI | PepMLM | 9.046337 |
| HMPV P | AAS22075.1 | HMPV_13 | KTLTEQQELLR | PepMLM | 9.120272 |
| HMPV P | AAS22075.1 | HMPV_14 | RLELTLEEQARLKL | PepMLM | 9.250608 |
| HMPV P | AAS22075.1 | HMPV_15 | PQRLRALELELRQQRRLL | PepMLM | 9.263967 |
| HMPV P | AAS22075.1 | HMPV_16 | EADALARLELLEAEARRLI | PepMLM | 9.290414 |
| HMPV P | AAS22075.1 | HMPV_17 | LLELELKKLTALAAKLI | PepMLM | 9.432891 |
| HMPV P | AAS22075.1 | HMPV_18 | ELELALEQLLR | PepMLM | 9.467909 |
| HMPV P | AAS22075.1 | HMPV_19 | PTEALAKLPTREALRKR | PepMLM | 9.484423 |
| HMPV P | AAS22075.1 | HMPV_20 | DLERLAASVLLEEARLKR | PepMLM | 9.516725 |
| Nipah virus P | AY029767.1 | NiV_1 | GKLLHHLLLQG | PepMLM | 4.69 |
| Nipah virus P | AY029767.1 | NiV_2 | SSKLLQLLLGN | PepMLM | 5.02 |

| | | | | | |
|---|---|---|---|---|---|
| Nipah virus P | AY029767.1 | NiV_3 | HHSLLHQLGLEG | PepMLM | 5.20 |
| Nipah virus P | AY029767.1 | NiV_4 | HSSLLQSLLLGG | PepMLM | 5.31 |
| Nipah virus P | AY029767.1 | NiV_5 | MQSVRLQLLLESLLK | PepMLM | 5.38 |
| Nipah virus P | AY029767.1 | NiV_6 | SHSLLQSLLQQG | PepMLM | 5.44 |
| Nipah virus P | AY029767.1 | NiV_7 | SSSLLHQLLQQG | PepMLM | 5.66 |
| Nipah virus P | AY029767.1 | NiV_8 | GHSLLQSLLLQG | PepMLM | 5.80 |
| Nipah virus P | AY029767.1 | NiV_9 | HSSLLLSLLQEG | PepMLM | 5.88 |
| Nipah virus P | AY029767.1 | NiV_10 | HSLLHQLLLKG | PepMLM | 5.90 |
| Nipah virus P | AY029767.1 | NiV_11 | SELLHRLLLEN | PepMLM | 6.08 |
| Nipah virus P | AY029767.1 | NiV_12 | HHSLLHSLLQEG | PepMLM | 6.19 |
| Nipah virus P | AY029767.1 | NiV_13 | HSSVLQLLLLEG | PepMLM | 6.44 |
| Nipah virus P | AY029767.1 | NiV_14 | GESVLQQLLQQGG | PepMLM | 6.50 |
| Nipah virus P | AY029767.1 | NiV_15 | SSSIPKQLRLESLKK | PepMLM | 6.69 |
| Nipah virus P | AY029767.1 | NiV_16 | HESLLQLLLEQG | PepMLM | 6.69 |
| Nipah virus P | AY029767.1 | NiV_17 | MSSVRKQLLLLLGLR | PepMLM | 6.75 |
| Nipah virus P | AY029767.1 | NiV_18 | SSLLLQLLLQN | PepMLM | 6.79 |
| Nipah virus P | AY029767.1 | NiV_19 | SSSLLQLLGQQG | PepMLM | 6.84 |
| Nipah virus P | AY029767.1 | NiV_20 | PSSVLLQLGLKE | PepMLM | 6.93 |

**Supplementary Table 5. RFDiffusion parameter setting used for generation of peptides for Figure 1.**

| Parameter | Setting |
|---|---|
| PDB | 7L0J:B |
| Contigs | B16-124:12-12 |
| Copies | 1 |
| Num_seqs | 4 |
| Initial guess | True |
| Use_multimer | False |
| Num_recycles | 3 |
| Rm_aa | C |
| Num_designs | 4 |
| Mpnn_sampling_temp | 0.1 |